

Complete 1-loop study of exclusive J/ψ and Υ photoproduction with full GPD evolution

**J.P. Lansberg with C. Flett, S. Nabeebaccus, M. Nefedov, P. Sznajder
and J. Wagner**

IJCLab Orsay – Paris-Saclay U. – CNRS

QCD Evolution 2024, 27–31 May 2024, University of Pavia, Italy



This project is supported by the European Union's Horizon 2020 research and innovation programme under Grant agreement no. 824093

Exclusive quarkonium photoproduction and GPDs

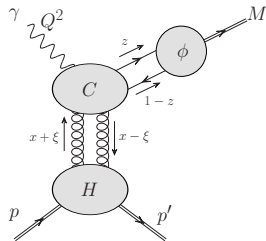
Collinear factorisation at the *amplitude* level:

$$\mathcal{A} = \int_{-1}^1 dx \int_0^1 dz H(x) \phi(z) C(x, z)$$

$H(x)$: Generalised parton distribution (GPD)

$\phi(z)$: Distribution amplitude

$C(x, z)$: Coefficient function



Exclusive quarkonium photoproduction and GPDs

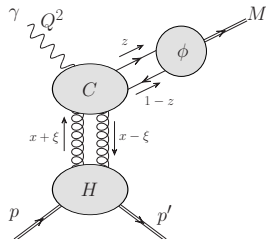
Collinear factorisation at the *amplitude* level:

$$\mathcal{A} = \int_{-1}^1 dx \int_0^1 dz H(x) \phi(z) C(x, z)$$

$H(x)$: Generalised parton distribution (GPD)

$\phi(z)$: Distribution amplitude

$C(x, z)$: Coefficient function



x : *Average* longitudinal momentum fraction of nucleon carried by the partons

- $H(x, \xi, t)$: Generalised (*3-dimensional*) parton distribution

ξ : *Longitudinal* momentum fraction *transferred* to hard part

t : momentum difference squared of nucleons

Exclusive quarkonium photoproduction and GPDs

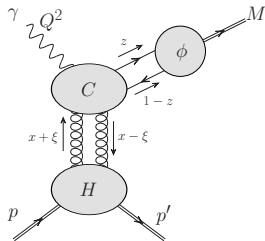
Collinear factorisation at the *amplitude* level:

$$\mathcal{A} = \int_{-1}^1 dx \int_0^1 dz H(x) \phi(z) C(x, z)$$

$H(x)$: Generalised parton distribution (GPD)

$\phi(z)$: Distribution amplitude

$C(x, z)$: Coefficient function



x : *Average* longitudinal momentum fraction of nucleon carried by the partons

- $H(x, \xi, t)$: Generalised (**3-dimensional**) parton distribution
 - ξ : *Longitudinal* momentum fraction *transferred* to hard part
 - t : momentum difference squared of nucleons

- GPDs reduce to PDFs in the **forward limit**:

$$H_q(x, 0, 0; \mu_F) = q(x; \mu_F), \quad H_g(x, 0, 0; \mu_F) = xg(x; \mu_F)$$

Exclusive quarkonium photoproduction and GPDs

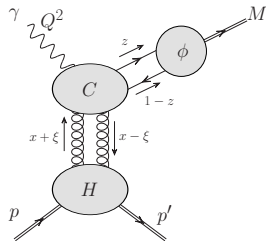
Collinear factorisation at the *amplitude* level:

$$\mathcal{A} = \int_{-1}^1 dx \int_0^1 dz H(x) \phi(z) C(x, z)$$

$H(x)$: Generalised parton distribution (GPD)

$\phi(z)$: Distribution amplitude

$C(x, z)$: Coefficient function



x : *Average* longitudinal momentum fraction of nucleon carried by the partons

- $H(x, \xi, t)$: Generalised (**3-dimensional**) parton distribution

ξ : *Longitudinal* momentum fraction *transferred* to hard part

t : momentum difference squared of nucleons

- GPDs reduce to PDFs in the **forward limit**:

$$H_q(x, 0, 0; \mu_F) = q(x; \mu_F), \quad H_g(x, 0, 0; \mu_F) = xg(x; \mu_F)$$

- No all-order proof of factorisation but correct IR-pole structure at **NLO**

[D. Ivanov, A. Schafer, L. Szymanowski, G. Krasnikov EPJC 34 (2004) 297]

Leading order amplitude

- Exclusive J/ψ photoproduction probes **gluon GPDs only** at LO.

Leading order amplitude

- Exclusive J/ψ photoproduction probes **gluon GPDs only** at **LO**.
- Employ *static limit* (NRQCD):
 $\implies \phi(z) \sim \delta(z - 1/2)$.

Leading order amplitude

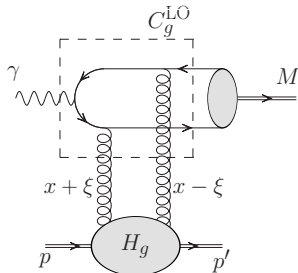
- Exclusive J/ψ photoproduction probes **gluon GPDs only** at LO.
- Employ **static limit** (NRQCD):
 $\implies \phi(z) \sim \delta(z - 1/2)$.

$$\mathcal{A} = \epsilon_\gamma^\mu \epsilon_M^{*\nu} \mathcal{T}^{\mu\nu}$$

$$\mathcal{T}_{\text{LO}}^{\mu\nu} = -g_\perp^{\mu\nu} \int_{-1}^1 \frac{dx}{x} \left[C_g^{\text{LO}} \left(\frac{\xi}{x} \right) \frac{H_g(x, \xi, \mu_F)}{x} \right]$$

$$C_g^{\text{LO}} \left(\frac{\xi}{x} \right) = \frac{F_{\text{LO}}}{\left[1 + \frac{\xi}{x} - i\delta \operatorname{sgn}(x) \right] \left[1 - \frac{\xi}{x} + i\delta \operatorname{sgn}(x) \right]}$$

$$F_{\text{LO}} = 4\pi\alpha_s e e_q \frac{2T_F}{N_c} \left(\frac{\langle \mathcal{O} [^3S_1^{[1]}] \rangle}{3m_c^3} \right)^{\frac{1}{2}}, \quad \xi = \frac{M^2}{2W_{\gamma p}^2 - M^2} \sim \frac{M^2}{2W_{\gamma p}^2}$$



Leading order amplitude

- Exclusive J/ψ photoproduction probes **gluon GPDs only** at LO.
- Employ **static limit** (NRQCD):
 $\implies \phi(z) \sim \delta(z - 1/2)$.

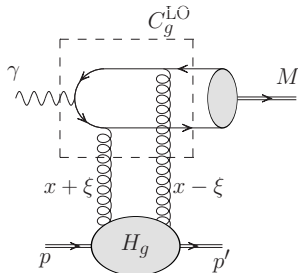
$$\mathcal{A} = \epsilon_\gamma^\mu \epsilon_M^{*\nu} \mathcal{T}^{\mu\nu}$$

$$\mathcal{T}_{\text{LO}}^{\mu\nu} = -g_\perp^{\mu\nu} \int_{-1}^1 \frac{dx}{x} \left[C_g^{\text{LO}} \left(\frac{\xi}{x} \right) \frac{H_g(x, \xi, \mu_F)}{x} \right]$$

$$C_g^{\text{LO}} \left(\frac{\xi}{x} \right) = \frac{F_{\text{LO}}}{\left[1 + \frac{\xi}{x} - i\delta \operatorname{sgn}(x) \right] \left[1 - \frac{\xi}{x} + i\delta \operatorname{sgn}(x) \right]}$$

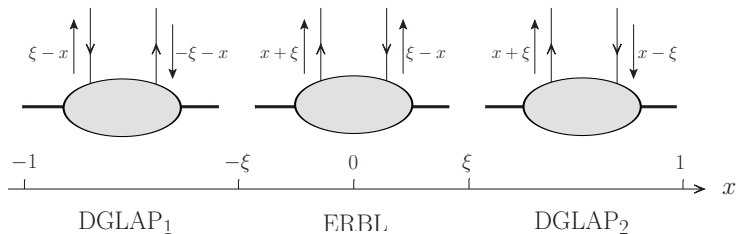
$$F_{\text{LO}} = 4\pi\alpha_s e e_q \frac{2T_F}{N_c} \left(\frac{\langle \mathcal{O} [^3S_1^{[1]}] \rangle}{3m_c^3} \right)^{\frac{1}{2}}, \quad \xi = \frac{M^2}{2W_{\gamma p}^2 - M^2} \sim \frac{M^2}{2W_{\gamma p}^2}$$

Large $W_{\gamma p}$ (small x in inclusive physics) \leftrightarrow **small ξ**



Imaginary part of amplitude

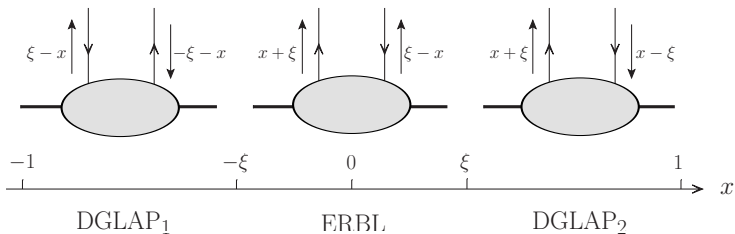
DGLAP and ERBL regions



- Evolution equations different in ERBL/DGLAP regions.

Imaginary part of amplitude

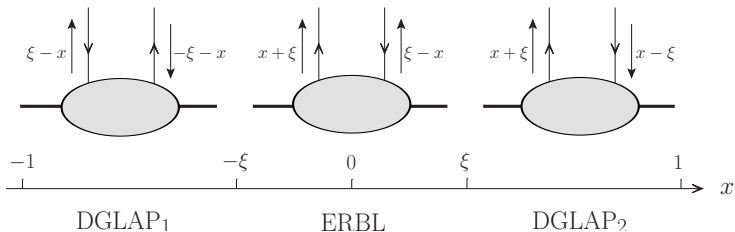
DGLAP and ERBL regions



- Evolution equations different in ERBL/DGLAP regions.
- ERBL region shrinks as $W_{\gamma p}$ increases.

Imaginary part of amplitude

DGLAP and ERBL regions



For LO amplitude:

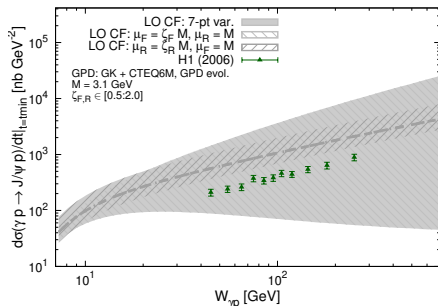
- Picks up *imaginary part* at $x = \pm \xi$.

$$\text{Im} C_g^{\text{LO}} \left(\frac{\xi}{x} \right) = -\pi \frac{F_{LO}}{2} \left[\delta \left(\frac{\xi}{x} - 1 \right) + \delta \left(\frac{\xi}{x} + 1 \right) \right]$$

$$\text{Im} \mathcal{T}_{\text{LO}}^{\mu\nu} = \pi \frac{g_{\perp}^{\mu\nu} F_{LO}}{\xi} H_g(\xi, \xi)$$

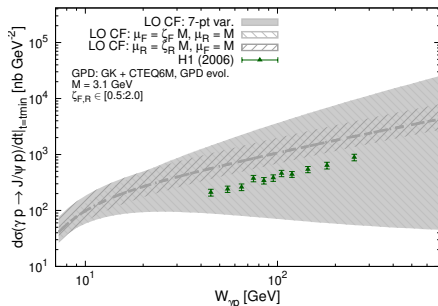
- Otherwise, amplitude fully real (principal value contribution).

LO cross section



Used GPDs are based on the *Goloskokov-Kroll model* EPJC 50 (2007) 829, i.e. Radyushkin's double-distribution with CTEQ6M as the input PDFs to construct the GPDs.

LO cross section

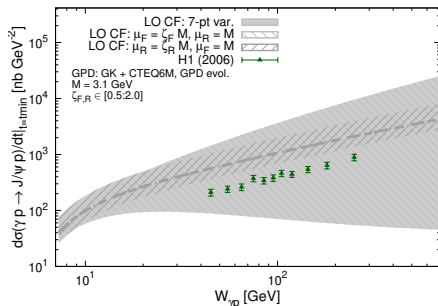


Used GPDs are based on the *Goloskokov-Kroll model* EPJC 50 (2007) 829, i.e. Radyushkin's double-distribution with CTEQ6M as the input PDFs to construct the GPDs.

Full LO evolution of GPDs is performed with APFEL++.

V. Bertone, H. Dutrieux, C. Mezrag, J. M. Morgado and H. Moutarde, EPJC 82 (2022) 888

LO cross section



Used GPDs are based on the *Goloskokov-Kroll model* EPJC 50 (2007) 829, i.e. Radyushkin's double-distribution with CTEQ6M as the input PDFs to construct the GPDs.

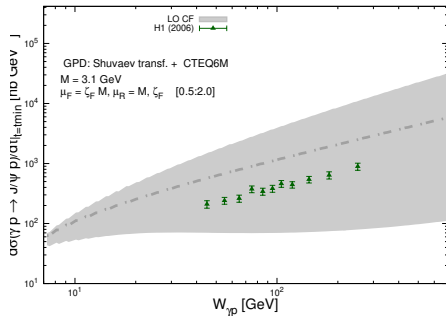
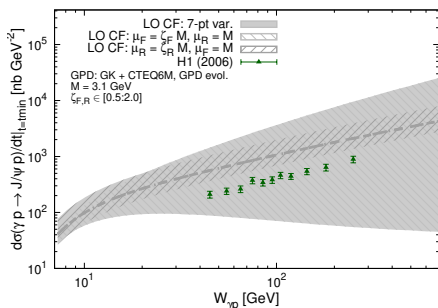
Full LO evolution of GPDs is performed with APFEL++.

V. Bertone, H. Dutrieux, C. Mezrag, J. M. Morgado and H. Moutarde, EPJC 82 (2022) 888

The W dependence of the lower bound is for $\mu_F = M/2$ and is due to an *unwanted feature of some gluon PDFs* at low scale with a local minimum at $x \approx 10^{-3}$!

see JPL, M.A. Ozcelik, EPJC 81 (2021) 497

LO cross section



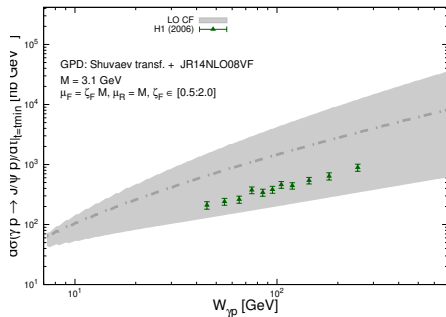
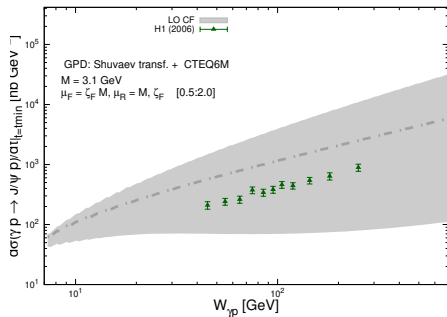
Used GPDs are based on the *Goloskokov-Kroll model* EPJC 50 (2007) 829, i.e. Radyushkin's double-distribution with CTEQ6M as the input PDFs to construct the GPDs.

Alternative (right) GPDs based on *Shuvaev transform* also using CTEQ6M

The W dependence of the lower bound is for $\mu_F = M/2$ and is due to an *unwanted feature of some gluon PDFs* at low scale with a local minimum at $x \approx 10^{-3}$!

see JPL, M.A. Ozcelik, EPJC 81 (2021) 497

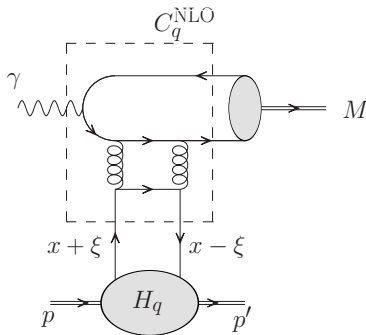
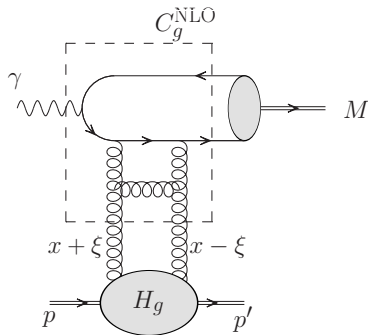
LO cross section



Weird behaviour absent with JR14 (right plot)

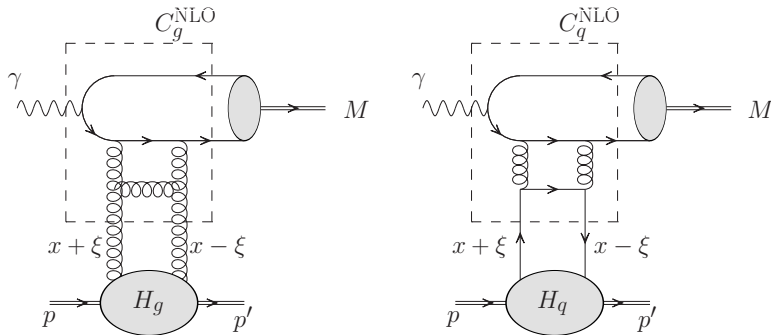
NLO amplitude

NLO amplitude has contributions from *both* quark and gluon GPDs:



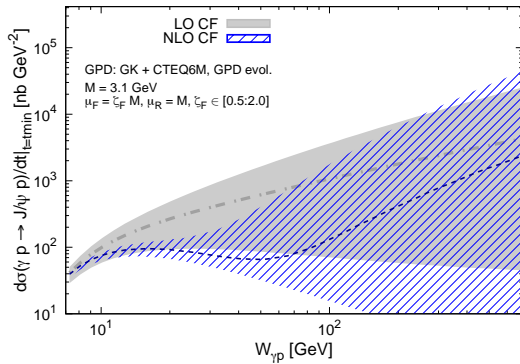
NLO amplitude

NLO amplitude has contributions from *both* quark and gluon GPDs:

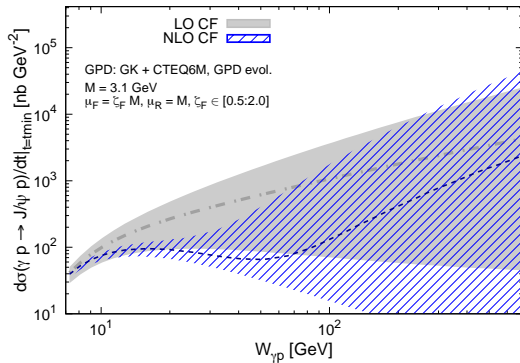


Imaginary part comes fully from the *DGLAP region* ($\xi \leq |x| \leq 1$)

NLO cross section

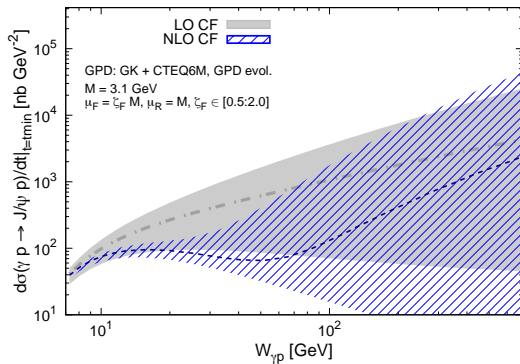


NLO cross section



Oscillating energy dependence combined with a fast increasing uncertainty

NLO cross section

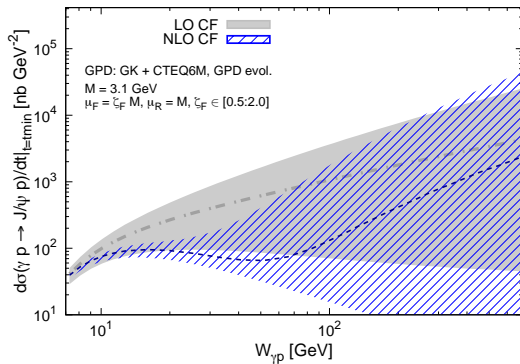


Oscillating energy dependence combined with a fast increasing uncertainty

Confirmation of an issue already uncovered twenty years ago

[D. Ivanov, A. Schafer, L. Szymanowski, G. Krasnikov EPJC 34 (2004) 297]

NLO cross section



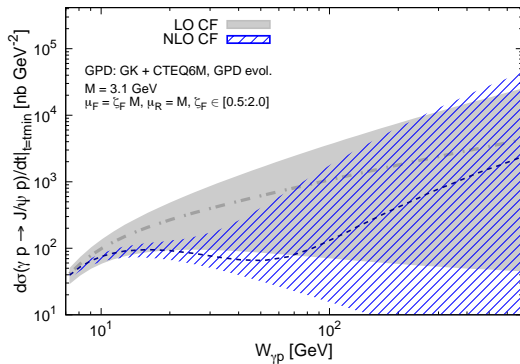
Oscillating energy dependence combined with a fast increasing uncertainty

Confirmation of an issue already uncovered twenty years ago

[D. Ivanov, A. Schafer, L. Szymanowski, G. Krasnikov EPJC 34 (2004) 297]

Already occurs at $W \approx 10 \sim 20$ GeV !

NLO cross section



Oscillating energy dependence combined with a fast increasing uncertainty

Confirmation of an issue already uncovered twenty years ago

[D. Ivanov, A. Schafer, L. Szymanowski, G. Krasnikov EPJC 34 (2004) 297]

Already occurs at $W \approx 10 \sim 20$ GeV !

how to solve this ?

Origin of the problem for NLO cross sections

$$\mathcal{T}_{\text{NLO}}^{\mu\nu} \supset i\pi \frac{g_{\perp}^{\mu\nu} F_{LO}}{\xi} \left[H_g(\xi, \xi) + \frac{\alpha_s(\mu_R) C_A}{\pi} \ln \left(\frac{M^2}{4\mu_F^2} \right) \int_{\xi}^1 \frac{dx}{x} H_g(x, \xi) \right. \\ \left. + \frac{\alpha_s(\mu_R) C_A}{\pi} \frac{C_F}{C_A} \ln \left(\frac{M^2}{4\mu_F^2} \right) \int_{\xi}^1 dx (H_q(x, \xi) - H_q(-x, \xi)) \right]$$

$H_g(x, \xi) \sim \text{const}$, as $x \rightarrow \xi$ for small ξ
 \implies appearance of $\ln \xi$ (high-energy logs).

Origin of the problem for NLO cross sections

$$\mathcal{T}_{\text{NLO}}^{\mu\nu} \supset i\pi \frac{g_{\perp}^{\mu\nu} F_{LO}}{\xi} \left[H_g(\xi, \xi) + \frac{\alpha_s(\mu_R) C_A}{\pi} \ln \left(\frac{M^2}{4\mu_F^2} \right) \int_{\xi}^1 \frac{dx}{x} H_g(x, \xi) \right. \\ \left. + \frac{\alpha_s(\mu_R) C_A}{\pi} \frac{C_F}{C_A} \ln \left(\frac{M^2}{4\mu_F^2} \right) \int_{\xi}^1 dx (H_q(x, \xi) - H_q(-x, \xi)) \right]$$

$H_g(x, \xi) \sim \text{const}$, as $x \rightarrow \xi$ for small ξ
 \implies appearance of $\ln \xi$ (high-energy logs).

Same thing happens in the quark case, since $H_q^{(+)}(x, \xi) \equiv H_q(x, \xi) - H_q(-x, \xi) \sim \frac{1}{x}$
 as $x, \xi \rightarrow 0$

Origin of the problem for NLO cross sections

$$\mathcal{T}_{\text{NLO}}^{\mu\nu} \supset i\pi \frac{g_{\perp}^{\mu\nu} F_{LO}}{\xi} \left[H_g(\xi, \xi) + \frac{\alpha_s(\mu_R) C_A}{\pi} \ln \left(\frac{M^2}{4\mu_F^2} \right) \int_{\xi}^1 \frac{dx}{x} H_g(x, \xi) \right. \\ \left. + \frac{\alpha_s(\mu_R) C_A}{\pi} \frac{C_F}{C_A} \ln \left(\frac{M^2}{4\mu_F^2} \right) \int_{\xi}^1 dx (H_q(x, \xi) - H_q(-x, \xi)) \right]$$

$H_g(x, \xi) \sim \text{const}$, as $x \rightarrow \xi$ for small ξ
 \implies appearance of $\ln \xi$ (high-energy logs).

Same thing happens in the quark case, since $H_q^{(+)}(x, \xi) \equiv H_q(x, \xi) - H_q(-x, \xi) \sim \frac{1}{x}$
 as $x, \xi \rightarrow 0$

Large $\ln \xi$ contributions are purely imaginary and come from the DGLAP region
 ($\xi < |x| < 1$).

Origin of the problem for NLO cross sections

$$\mathcal{T}_{\text{NLO}}^{\mu\nu} \supset i\pi \frac{g_{\perp}^{\mu\nu} F_{LO}}{\xi} \left[H_g(\xi, \xi) + \frac{\alpha_s(\mu_R) C_A}{\pi} \ln \left(\frac{M^2}{4\mu_F^2} \right) \int_{\xi}^1 \frac{dx}{x} H_g(x, \xi) \right. \\ \left. + \frac{\alpha_s(\mu_R) C_A}{\pi} \frac{C_F}{C_A} \ln \left(\frac{M^2}{4\mu_F^2} \right) \int_{\xi}^1 dx (H_q(x, \xi) - H_q(-x, \xi)) \right]$$

$H_g(x, \xi) \sim \text{const}$, as $x \rightarrow \xi$ for small ξ
 \implies appearance of $\ln \xi$ (high-energy logs).

Same thing happens in the quark case, since $H_q^{(+)}(x, \xi) \equiv H_q(x, \xi) - H_q(-x, \xi) \sim \frac{1}{x}$
 as $x, \xi \rightarrow 0$

Large $\ln \xi$ contributions are purely imaginary and come from the DGLAP region ($\xi < |x| < 1$).

NLO correction of opposite sign to LO for $\mu_F = M (> M/2)$
cancellation then strong μ_F dependence at large W

Why large scale uncertainties present?

In the DGLAP evolution of low ξ GPDs, the probability of emitting a new gluon is *strongly enhanced* by the large value of $\ln \xi$.

Why large scale uncertainties present?

In the DGLAP evolution of low ξ GPDs, the probability of emitting a new gluon is *strongly enhanced* by the large value of $\ln \xi$.

In contrast, the NLO coefficient function allows for the emission (and reabsorption) of *only one gluon*.

Why large scale uncertainties present?

In the DGLAP evolution of low ξ GPDs, the probability of emitting a new gluon is *strongly enhanced* by the large value of $\ln \xi$.

In contrast, the NLO coefficient function allows for the emission (and reabsorption) of *only one gluon*.

⇒ we cannot expect compensation between the contributions coming from the GPD and the coefficient function as we vary the scale μ_F .

Why large scale uncertainties present?

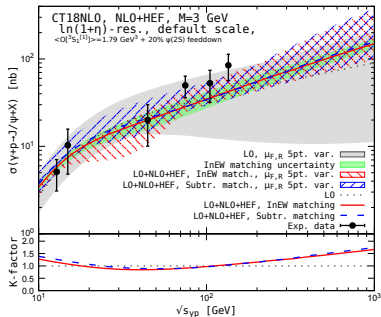
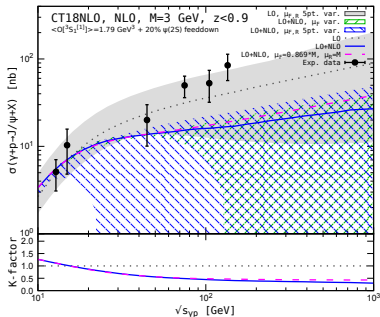
In the DGLAP evolution of low ξ GPDs, the probability of emitting a new gluon is *strongly enhanced* by the large value of $\ln \xi$.

In contrast, the NLO coefficient function allows for the emission (and reabsorption) of *only one gluon*.

⇒ we cannot expect compensation between the contributions coming from the GPD and the coefficient function as we vary the scale μ_F .

⇒ Hints towards a solution through *resummation* of these logarithms...

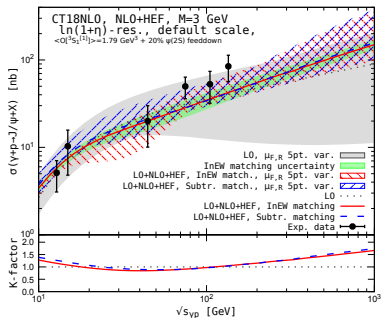
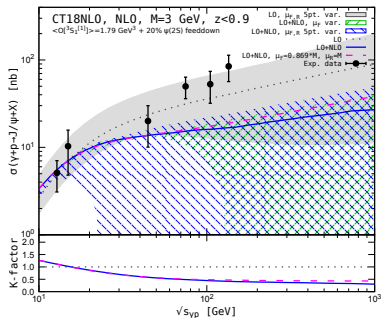
Instabilities in inclusive cases, e.g. $\gamma p \rightarrow Q + X$



Perturbative instabilities leading to negative cross sections in inclusive quarkonium production known since 90's:

- hadroproduction of η_c and χ_c
- photoproduction of J/ψ

Instabilities in inclusive cases, e.g. $\gamma p \rightarrow Q + X$



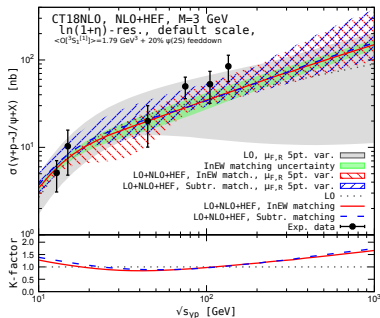
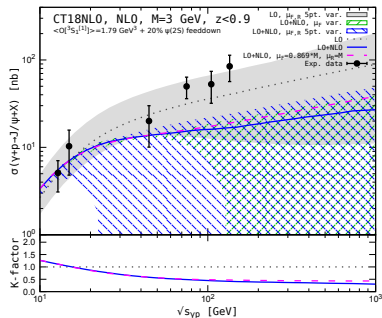
Perturbative instabilities leading to negative cross sections in inclusive quarkonium production known since 90's:

- hadroproduction of η_c and χ_c
- photoproduction of J/ψ

Understood recently; first solution via *scale fixing*

JPL, M.A. Ozcelik, EPJC 81 (2021) 6, 497; A. Colpani Serri et al. PLB 835 (2022) 137556

Instabilities in inclusive cases, e.g. $\gamma p \rightarrow Q + X$



Perturbative instabilities leading to negative cross sections in inclusive quarkonium production known since 90's:

- hadroproduction of η_c and χ_c
- photoproduction of J/ψ

Understood recently; first solution via *scale fixing*

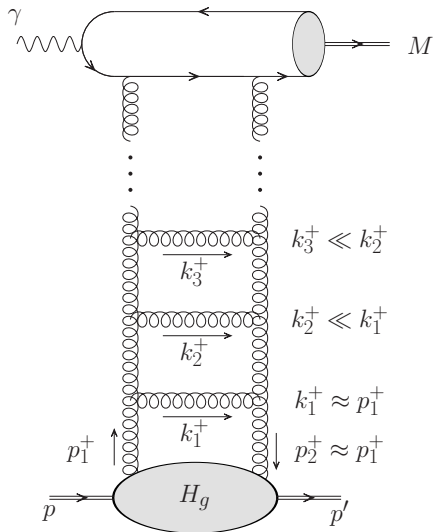
JPL, M.A. Ozcelik, EPJC 81 (2021) 6, 497; A. Colpani Serri et al. PLB 835 (2022) 137556

Solved by matching High Energy Factorisation (HEF) to Collinear Factorisation

J.P. Lansberg, M. Nefedov, M.A. Ozcelik, JHEP 05 (2022) 083 & EPJC 84 (2024) 351

Multiple gluon emissions:

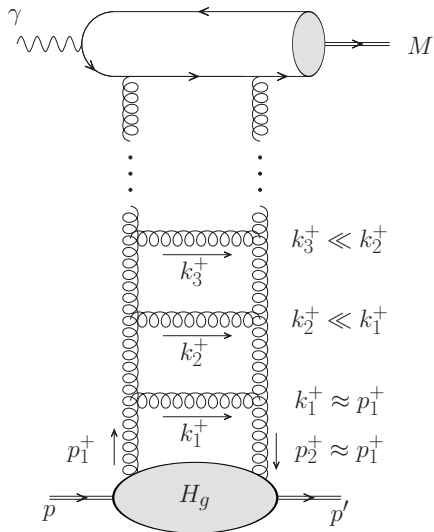
BFKL ladder and resummation



- Logarithms are generated by emission of gluons, with **strong ordering in + lightcone momentum**.

Multiple gluon emissions:

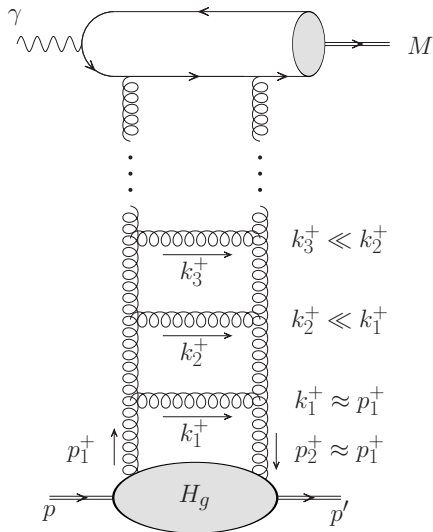
BFKL ladder and resummation



- Logarithms are generated by emission of gluons, with **strong ordering in + lightcone momentum**.
- They become **large at high energies**, and need to be **resummed**.

Multiple gluon emissions:

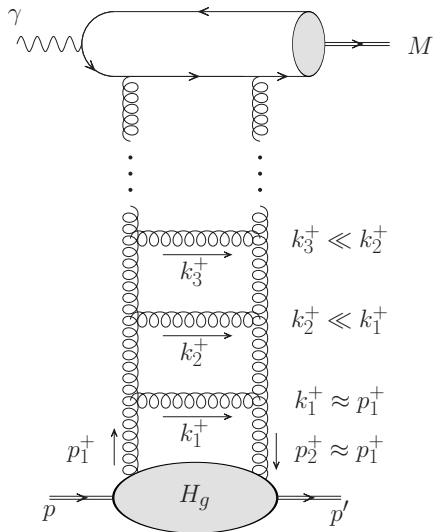
BFKL ladder and resummation



- Logarithms are generated by emission of gluons, with **strong ordering in + lightcone momentum**.
- They become **large at high energies**, and need to be **resummed**.
- We implement a **resummation** of these BFKL-type logs using HEF, consistent with **fixed-order evolution of GPD**:

Multiple gluon emissions:

BFKL ladder and resummation



- Logarithms are generated by emission of gluons, with **strong ordering in + lightcone momentum**.
- They become **large at high energies**, and need to be **resummed**.
- We implement a **resummation** of these BFKL-type logs using HEF, consistent with **fixed-order evolution of GPD**:
 \implies **Doubly-logarithmic approximation (DLA)**

Implementation of resummation: $C^{\text{CF}} \rightarrow C^{\text{HEF}}$

$$C_g^{\text{HEF}}\left(\frac{\xi}{x}\right) = \frac{-i\pi\hat{\alpha}_s F_{\text{LO}}}{2\left|\frac{\xi}{x}\right|} \sqrt{\frac{L_\mu}{L_x}} \left\{ I_1\left(2\sqrt{L_x L_\mu}\right) - 2 \sum_{k=1}^{\infty} \text{Li}_{2k}(-1) \left(\frac{L_x}{L_\mu}\right)^k I_{2k-1}\left(2\sqrt{L_x L_\mu}\right) \right\},$$

where $L_\mu = \ln[M^2/(4\mu_F^2)]$, $L_x = \hat{\alpha}_s \ln\left|\frac{x}{\xi}\right|$ and $\hat{\alpha}_s = \alpha_s(\mu_R)C_A/\pi$.

Implementation of resummation: $C^{\text{CF}} \rightarrow C^{\text{HEF}}$

$$C_g^{\text{HEF}}\left(\frac{\xi}{x}\right) = \frac{-i\pi\hat{\alpha}_s F_{\text{LO}}}{2\left|\frac{\xi}{x}\right|} \sqrt{\frac{L_\mu}{L_x}} \left\{ I_1\left(2\sqrt{L_x L_\mu}\right) - 2 \sum_{k=1}^{\infty} \text{Li}_{2k}(-1) \left(\frac{L_x}{L_\mu}\right)^k I_{2k-1}\left(2\sqrt{L_x L_\mu}\right) \right\},$$

where $L_\mu = \ln[M^2/(4\mu_F^2)]$, $L_x = \hat{\alpha}_s \ln\left|\frac{x}{\xi}\right|$ and $\hat{\alpha}_s = \alpha_s(\mu_R) C_A/\pi$.

This yields, when expanded in α_s ,

$$C_g^{\text{HEF}}\left(\frac{\xi}{x}\right) = \frac{-i\pi F_{\text{LO}}}{2} \underbrace{\left(\delta\left(\left|\frac{\xi}{x}\right| - 1\right) + \frac{\hat{\alpha}_s}{\left|\frac{\xi}{x}\right|} \ln\left(\frac{M^2}{4\mu_F^2}\right) \right)}_{\rightarrow C_g^{\text{asy}}} + \frac{\hat{\alpha}_s^2}{\left|\frac{\xi}{x}\right|} \ln\frac{1}{\left|\frac{\xi}{x}\right|} \left[\frac{\pi^2}{6} + \frac{1}{2} \ln^2\left(\frac{M^2}{4\mu_F^2}\right) \right] + \dots$$

- First two terms in α_s corresponds to the LO/NLO CF computation at small x .

Implementation of resummation: $C^{\text{CF}} \rightarrow C^{\text{HEF}}$

$$C_g^{\text{HEF}}\left(\frac{\xi}{x}\right) = \frac{-i\pi\hat{\alpha}_s F_{\text{LO}}}{2\left|\frac{\xi}{x}\right|} \sqrt{\frac{L_\mu}{L_x}} \left\{ h_1\left(2\sqrt{L_x L_\mu}\right) - 2 \sum_{k=1}^{\infty} \text{Li}_{2k}(-1) \left(\frac{L_x}{L_\mu}\right)^k I_{2k-1}\left(2\sqrt{L_x L_\mu}\right) \right\},$$

where $L_\mu = \ln[M^2/(4\mu_F^2)]$, $L_x = \hat{\alpha}_s \ln\left|\frac{x}{\xi}\right|$ and $\hat{\alpha}_s = \alpha_s(\mu_R) C_A/\pi$.

This yields, when expanded in α_s ,

$$C_g^{\text{HEF}}\left(\frac{\xi}{x}\right) = \frac{-i\pi F_{\text{LO}}}{2} \underbrace{\left(\delta\left(\left|\frac{\xi}{x}\right| - 1\right) + \frac{\hat{\alpha}_s}{\left|\frac{\xi}{x}\right|} \ln\left(\frac{M^2}{4\mu_F^2}\right) + \frac{\hat{\alpha}_s^2}{\left|\frac{\xi}{x}\right|} \ln\frac{1}{\left|\frac{\xi}{x}\right|} \left[\frac{\pi^2}{6} + \frac{1}{2} \ln^2\left(\frac{M^2}{4\mu_F^2}\right) \right] + \dots \right)}_{\rightarrow C_g^{\text{asy}}},$$

- First two terms in α_s corresponds to the LO/NLO CF computation at small x .
- *Cannot use scale fixing at NNLO to get rid of all the $1/\xi$ -enhanced contributions*

Implementation of resummation: $C^{\text{CF}} \rightarrow C^{\text{HEF}}$

$$C_g^{\text{HEF}}\left(\frac{\xi}{x}\right) = \frac{-i\pi\hat{\alpha}_s F_{\text{LO}}}{2\left|\frac{\xi}{x}\right|} \sqrt{\frac{L_\mu}{L_x}} \left\{ h_1\left(2\sqrt{L_x L_\mu}\right) - 2 \sum_{k=1}^{\infty} \text{Li}_{2k}(-1) \left(\frac{L_x}{L_\mu}\right)^k I_{2k-1}\left(2\sqrt{L_x L_\mu}\right) \right\},$$

where $L_\mu = \ln[M^2/(4\mu_F^2)]$, $L_x = \hat{\alpha}_s \ln\left|\frac{x}{\xi}\right|$ and $\hat{\alpha}_s = \alpha_s(\mu_R) C_A/\pi$.

This yields, when expanded in α_s ,

$$C_g^{\text{HEF}}\left(\frac{\xi}{x}\right) = \frac{-i\pi F_{\text{LO}}}{2} \underbrace{\left(\delta\left(\left|\frac{\xi}{x}\right| - 1\right) + \frac{\hat{\alpha}_s}{\left|\frac{\xi}{x}\right|} \ln\left(\frac{M^2}{4\mu_F^2}\right) + \frac{\hat{\alpha}_s^2}{\left|\frac{\xi}{x}\right|} \ln\frac{1}{\left|\frac{\xi}{x}\right|} \left[\frac{\pi^2}{6} + \frac{1}{2} \ln^2\left(\frac{M^2}{4\mu_F^2}\right) \right] + \dots \right)}_{\rightarrow C_g^{\text{asy}}},$$

- First two terms in α_s corresponds to the LO/NLO CF computation at small x .
- *Cannot use scale fixing at NNLO to get rid of all the $1/\xi$ -enhanced contributions*

Quark coefficient function:

$$C_q^{\text{HEF}}\left(\frac{\xi}{x}\right) = \frac{2C_F}{C_A} C_g^{\text{HEF}}\left(\frac{\xi}{x}\right),$$

Matching

We use *subtractive matching*:

$$\begin{aligned}
 C_{g,q}^{\text{match.}} \left(\frac{\tilde{\zeta}}{x} \right) &= C_{g,q}^{\text{NLO CF}} \left(\frac{\tilde{\zeta}}{x} \right) - C_{g,q}^{\text{asy.}} \left(\frac{\tilde{\zeta}}{x} \right) + C_{g,q}^{\text{HEF}} \left(\frac{\tilde{\zeta}}{x} \right), \\
 C_g^{\text{asy.}} \left(\frac{\tilde{\zeta}}{x} \right) &= \frac{C_A}{2C_F} C_q^{\text{asy.}} \left(\frac{\tilde{\zeta}}{x} \right) \\
 &= \frac{-i\pi F_{\text{LO}}}{2} \left[\delta \left(\left| \frac{\tilde{\zeta}}{x} \right| - 1 \right) + \frac{\hat{\alpha}_s}{\left| \frac{\tilde{\zeta}}{x} \right|} \ln \left(\frac{M^2}{4\mu_F^2} \right) \right].
 \end{aligned}$$

- $C_g^{\text{asy.}} \left(\frac{\tilde{\zeta}}{x} \right)$: first two terms in the α_s expansion of $C_g^{\text{HEF}} \left(\frac{\tilde{\zeta}}{x} \right)$.

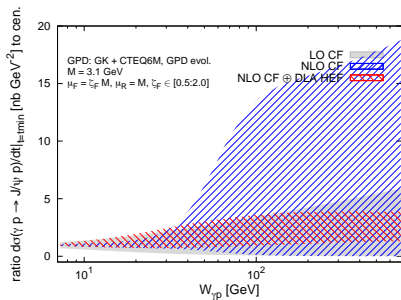
Matching

We use *subtractive matching*:

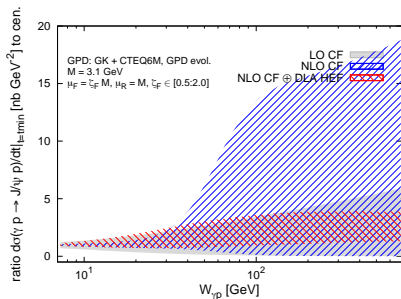
$$\begin{aligned}
 C_{g,q}^{\text{match.}} \left(\frac{\tilde{\zeta}}{x} \right) &= C_{g,q}^{\text{NLO CF}} \left(\frac{\tilde{\zeta}}{x} \right) - C_{g,q}^{\text{asy.}} \left(\frac{\tilde{\zeta}}{x} \right) + C_{g,q}^{\text{HEF}} \left(\frac{\tilde{\zeta}}{x} \right), \\
 C_g^{\text{asy.}} \left(\frac{\tilde{\zeta}}{x} \right) &= \frac{C_A}{2C_F} C_q^{\text{asy.}} \left(\frac{\tilde{\zeta}}{x} \right) \\
 &= \frac{-i\pi F_{\text{LO}}}{2} \left[\delta \left(\left| \frac{\tilde{\zeta}}{x} \right| - 1 \right) + \frac{\hat{\alpha}_s}{\left| \frac{\tilde{\zeta}}{x} \right|} \ln \left(\frac{M^2}{4\mu_F^2} \right) \right].
 \end{aligned}$$

- $C_g^{\text{asy.}} \left(\frac{\tilde{\zeta}}{x} \right)$: first two terms in the α_s expansion of $C_g^{\text{HEF}} \left(\frac{\tilde{\zeta}}{x} \right)$.
- Matching performed **before** x -integration.

Results: scale uncertainties for J/ψ



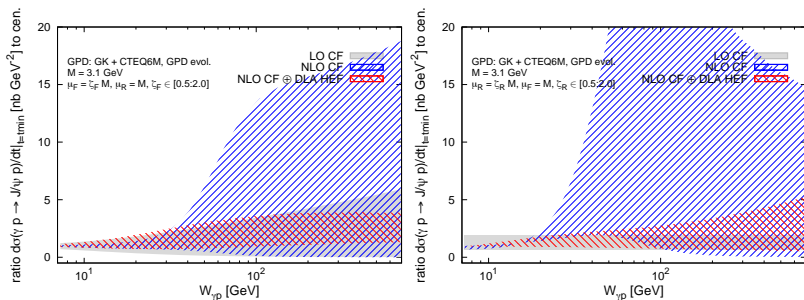
Results: scale uncertainties for J/ψ



- μ_F uncertainties (left)

- NLO CF \oplus DLA HEF much better than the pathological NLO CF
- NLO CF \oplus DLA HEF significantly better than LO CF, even at large W

Results: scale uncertainties for J/ψ



- μ_F uncertainties (left)

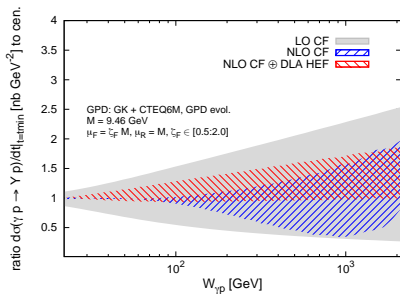
- NLO CF \oplus DLA HEF much better than the pathological NLO CF
- NLO CF \oplus DLA HEF significantly better than LO CF, even at large W

- μ_R uncertainties (right)

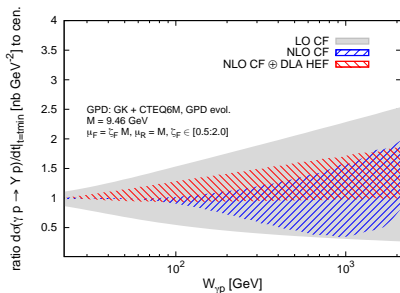
- NLO CF \oplus DLA HEF much better than the pathological NLO CF
- NLO CF \oplus DLA HEF gets worse at high energies compared to LO CF

[at large W , $\propto W^{\alpha_s(\mu_R)}$]

Results: scale uncertainties for Υ



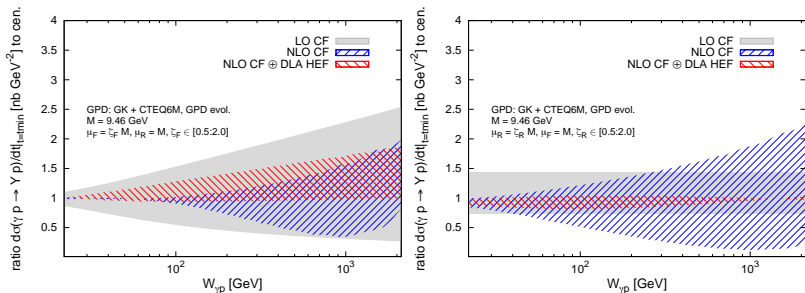
Results: scale uncertainties for Υ



- μ_F uncertainties (left)

- NLO CF \oplus DLA HEF much better than the pathological NLO CF
- NLO CF \oplus DLA HEF also much better than LO CF, even at large W

Results: scale uncertainties for Υ



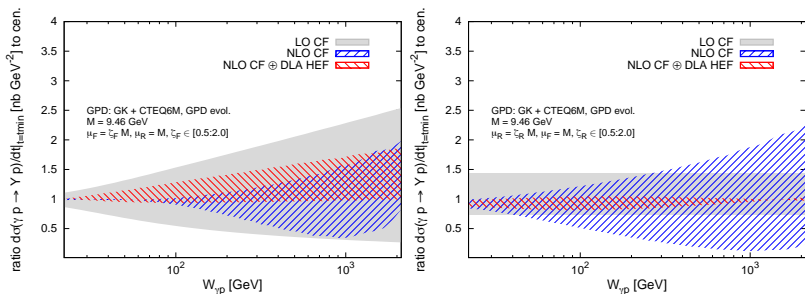
- μ_F uncertainties (left)

- NLO CF \oplus DLA HEF much better than the pathological NLO CF
- NLO CF \oplus DLA HEF also much better than LO CF, even at large W

- μ_R uncertainties (right)

- NLO CF \oplus DLA HEF much better than the pathological NLO CF
- NLO CF \oplus DLA HEF better than LO CF up to UPC LHC energies ($\mathcal{O}(1 \text{ TeV})$)

Results: scale uncertainties for Y



- μ_F uncertainties (left)

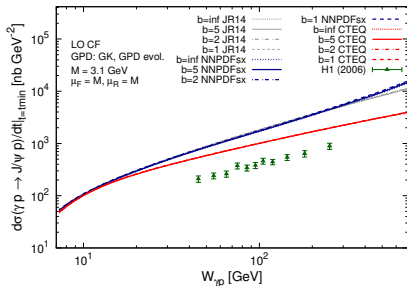
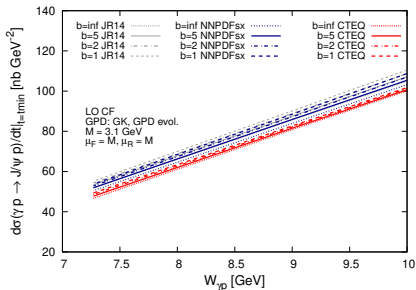
- NLO CF \oplus DLA HEF much better than the pathological NLO CF
- NLO CF \oplus DLA HEF also much better than LO CF, even at large W

- μ_R uncertainties (right)

- NLO CF \oplus DLA HEF much better than the pathological NLO CF
- NLO CF \oplus DLA HEF better than LO CF up to UPC LHC energies ($\mathcal{O}(1 \text{ TeV})$)

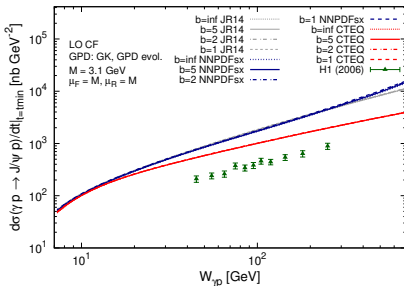
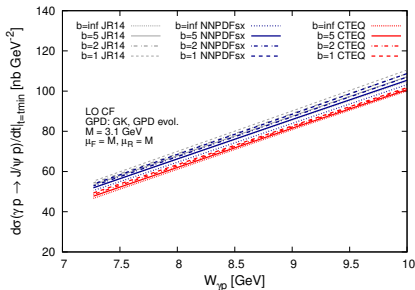
Perturbative instabilities are also present for Y !

Results: comparing different GPD inputs for LO CF



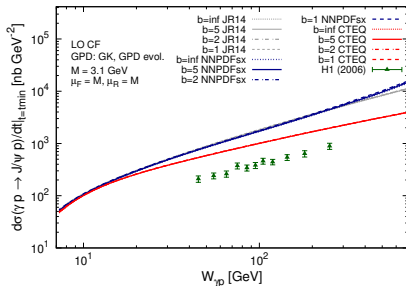
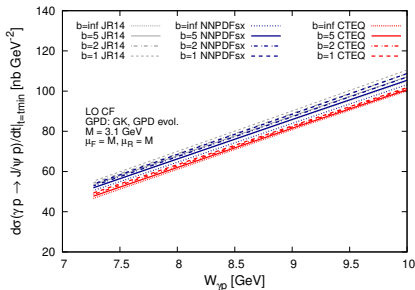
- GPD with PDF input using CTEQ6 (like GK) and 2 more modern PDFs not showing a dip (JR14 and NNPDFsx)
- Strength of ξ dependence of GPD from Double Distribution encoded in b

Results: comparing different GPD inputs for LO CF



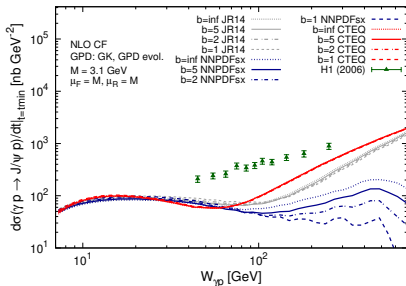
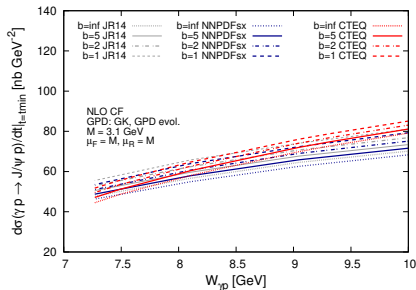
- GPD with PDF input using CTEQ6 (like GK) and 2 more modern PDFs not showing a dip (JR14 and NNPDFsx)
- Strength of ξ dependence of GPD from Double Distribution encoded in b
- Low energies (left)
 - Slight effect from b variation but smaller than changing PDFs
 - Also much smaller than scale uncertainties (previous slides)

Results: comparing different GPD inputs for LO CF



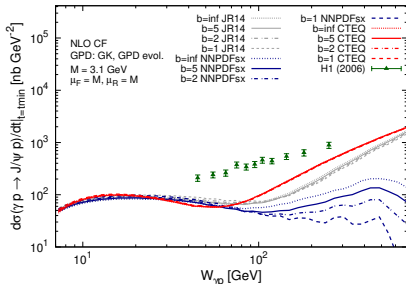
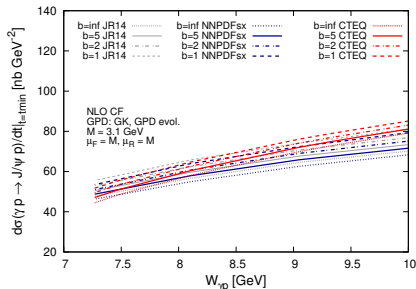
- GPD with PDF input using CTEQ6 (like GK) and 2 more modern PDFs not showing a dip (JR14 and NNPDFsx)
- Strength of ξ dependence of GPD from Double Distribution encoded in b
- Low energies (left)
 - Slight effect from b variation but smaller than changing PDFs
 - Also much smaller than scale uncertainties (previous slides)
- Higher energies (right) [log plot]
 - Effect from b variation negligible

Different GPD inputs for NLO CF



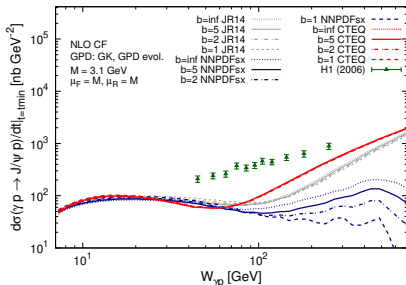
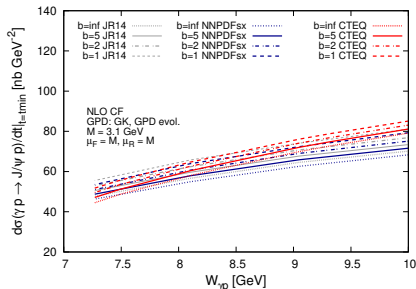
- GPD with PDF input using CTEQ6 (like GK) and 2 more modern PDFs not showing a dip (JR14 and NNPDFsx)
- Strength of ξ dependence of GPD from Double Distribution encoded in b

Different GPD inputs for NLO CF



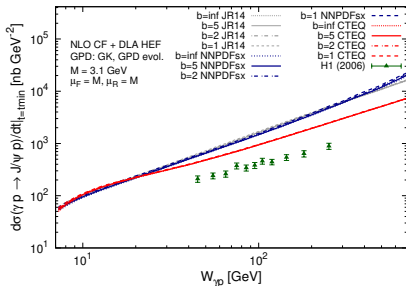
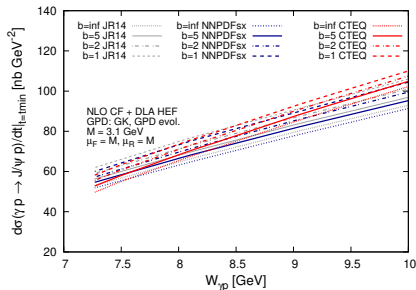
- GPD with PDF input using CTEQ6 (like GK) and 2 more modern PDFs not showing a dip (JR14 and NNPDFsx)
- Strength of ξ dependence of GPD from Double Distribution encoded in b
- Low energies (left)
 - Similar observations than for LO

Different GPD inputs for NLO CF



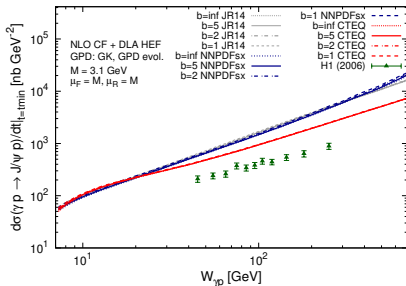
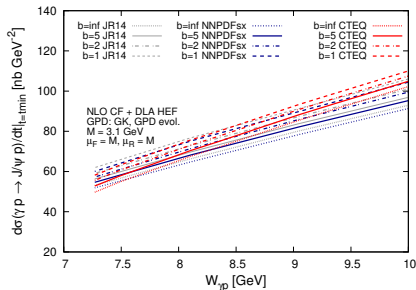
- GPD with PDF input using CTEQ6 (like GK) and 2 more modern PDFs not showing a dip (JR14 and NNPDFsx)
- Strength of ξ dependence of GPD from Double Distribution encoded in b
- Low energies (left)
 - Similar observations than for LO
- Higher energies (right) [log plot]
 - NLO results out of control at higher energies

Different GPD inputs for NLO CF \oplus HEF DLA



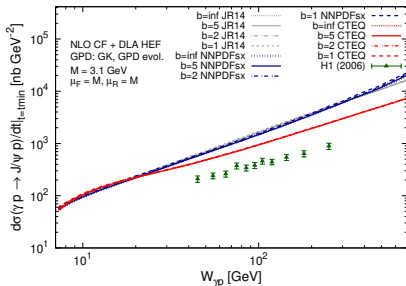
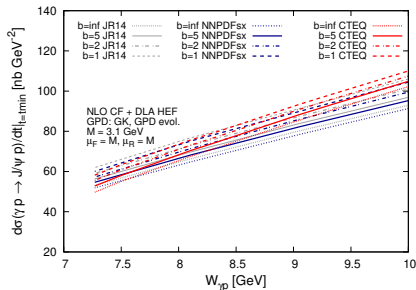
- GPD with PDF input using CTEQ6 (like GK) and 2 more modern PDFs not showing a dip (JR14 and NNPDFsx)
- Strength of ξ dependence of GPD from Double Distribution encoded in b

Different GPD inputs for NLO CF \oplus HEF DLA



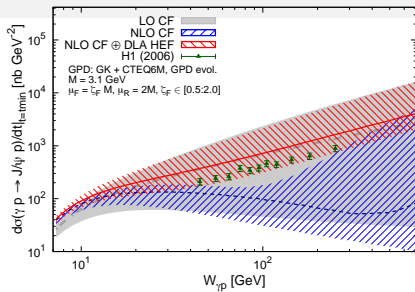
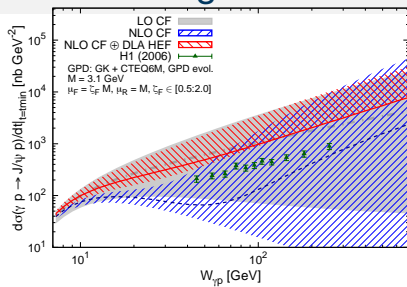
- GPD with PDF input using CTEQ6 (like GK) and 2 more modern PDFs not showing a dip (JR14 and NNPDFsx)
- Strength of ξ dependence of GPD from Double Distribution encoded in b
- Low energies (left)
 - Slight effect from b variation but smaller than changing PDFs
 - Also much smaller than scale uncertainties (previous slides)

Different GPD inputs for NLO CF \oplus HEF DLA

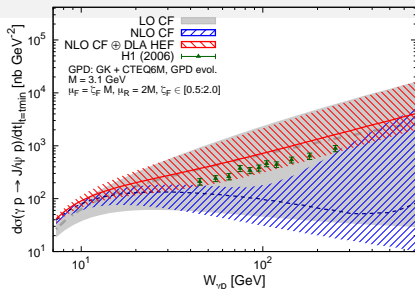
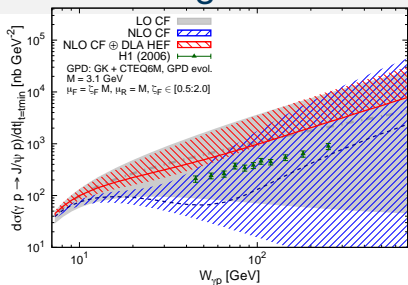


- GPD with PDF input using CTEQ6 (like GK) and 2 more modern PDFs not showing a dip (JR14 and NNPDFsx)
- Strength of ξ dependence of GPD from Double Distribution encoded in b
- Low energies (left)
 - Slight effect from b variation but smaller than changing PDFs
 - Also much smaller than scale uncertainties (previous slides)
- Higher energies (right) [log plot]
 - Effect from b variation negligible

Summarising our results

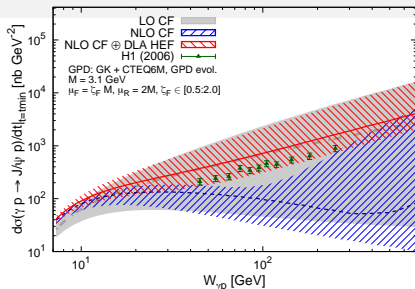
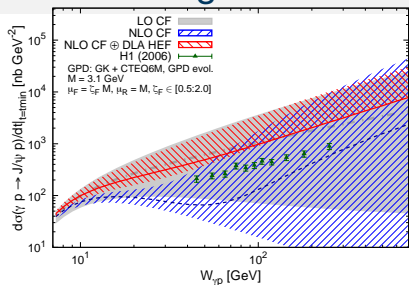


Summarising our results



- **NLO CF \oplus HEF DLA** cures the instabilities of NLO CF

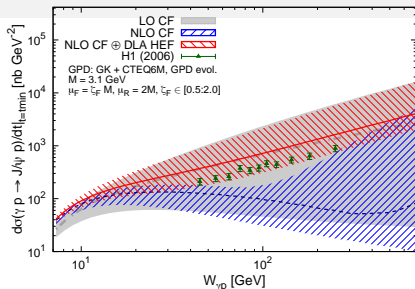
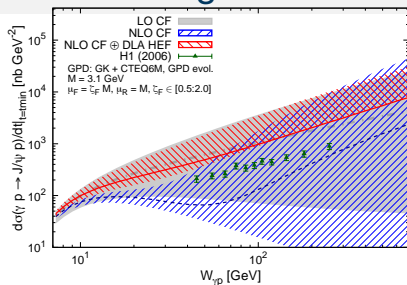
Summarising our results



- **NLO CF \oplus HEF DLA** cures the instabilities of NLO CF
- Theory in the ballpark of the H1 data, but clearly less precise

We only considered data at small t

Summarising our results

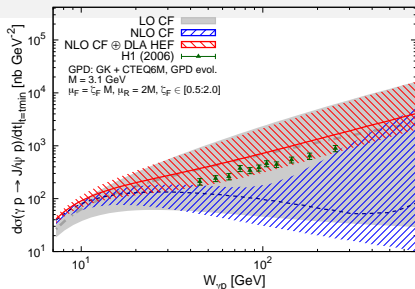
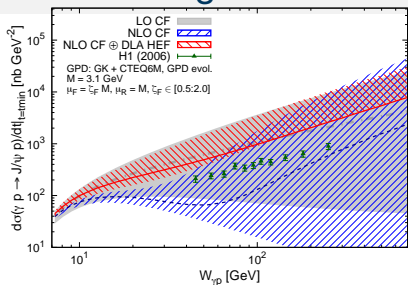


- **NLO CF \oplus HEF DLA** cures the instabilities of NLO CF
- Theory in the ballpark of the H1 data, but clearly less precise

We only considered data at small t

- A priori *better agreement if $\mu_R \approx 2M$* (right plot) but

Summarising our results



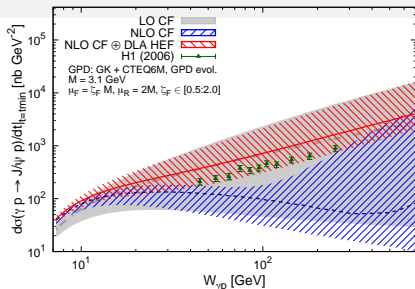
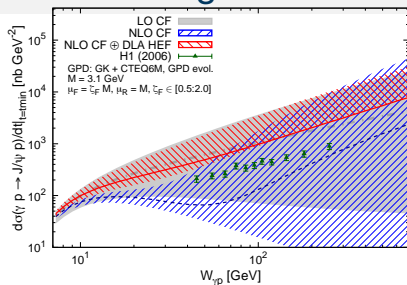
- **NLO CF \oplus HEF DLA** cures the instabilities of NLO CF
- Theory in the ballpark of the H1 data, but clearly less precise

We only considered data at small t

- A priori **better agreement if $\mu_R \approx 2M$** (right plot) but
- Impact of x/ζ GPD dependence unclear; varying b has negligible effect

Going beyond DD ?

Summarising our results



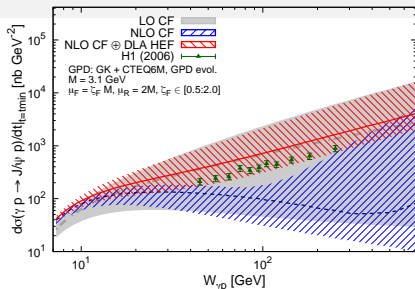
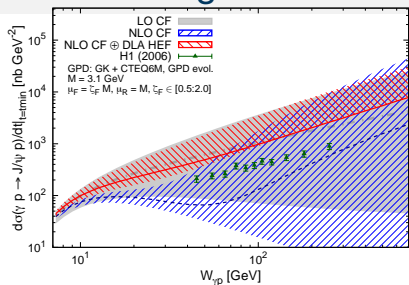
- **NLO CF \oplus HEF DLA** cures the instabilities of NLO CF
- Theory in the ballpark of the H1 data, but clearly less precise

We only considered data at small t

- A priori **better agreement if $\mu_R \approx 2M$** (right plot) but
 - Impact of x/ζ GPD dependence unclear; varying b has negligible effect
 - Impact of DA (relativistic corrections) vs strict static limit of NRQCD ?

Going beyond DD ?

Summarising our results



- ***NLO CF ⊕ HEF DLA*** cures the instabilities of NLO CF
- Theory in the ballpark of the H1 data, but clearly less precise

We only considered data at small t

- A priori *better agreement if $\mu_R \approx 2M$* (right plot) but

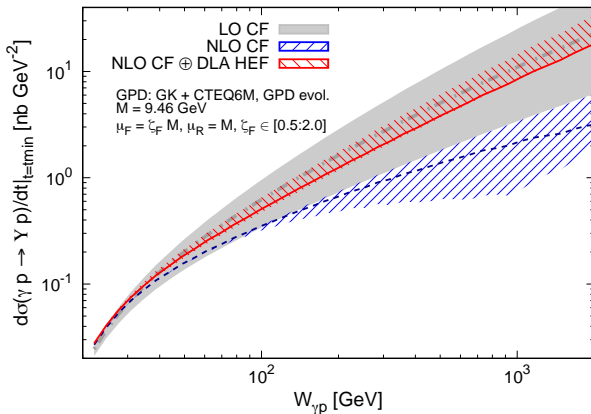
- Impact of x/ζ GPD dependence unclear; varying b has negligible effect

Going beyond DD ?

- Impact of DA (relativistic corrections) vs strict static limit of NRQCD ?
- Now ready for a full PDF uncertainty study

Only comparisons of central PDFs

Results for exclusive Υ photoproduction



- GPD based on CTEQ6M PDF input, *full LO evolution of GPDs*
- Significant corrections wrt NLO and reduction of the uncertainties
- Extrapolating $d\sigma/dt|_{t=t_{\min}}$ from measurements at $W = 100$ GeV, one gets 0.7 nb GeV^{-2} in agreement with the red band

ZEUS PLB 680 (2009) 4

Conclusion

- Exclusive J/ψ and Υ photoproduction at increasing $W_{\gamma p}$ suffers from *perturbative instabilities at NLO*.

Conclusion

- Exclusive J/ψ and Υ photoproduction at increasing $W_{\gamma p}$ suffers from *perturbative instabilities at NLO*.
- Similar situation to **inclusive** photoproduction and hadroproduction.

Conclusion

- Exclusive J/ψ and Υ photoproduction at increasing $W_{\gamma p}$ suffers from *perturbative instabilities at NLO*.
- Similar situation to **inclusive** photoproduction and hadroproduction.
- *Scale fixing* cures the issue at NLO, but *insufficient* beyond NLO.

Conclusion

- Exclusive J/ψ and Υ photoproduction at increasing $W_{\gamma p}$ suffers from *perturbative instabilities at NLO*.
- Similar situation to **inclusive** photoproduction and hadroproduction.
- *Scale fixing* cures the issue at NLO, but *insufficient* beyond NLO.
- First NLO study with GPD evolution done with APFEL++

Conclusion

- Exclusive J/ψ and Υ photoproduction at increasing $W_{\gamma p}$ suffers from *perturbative instabilities at NLO*.
- Similar situation to **inclusive** photoproduction and hadroproduction.
- *Scale fixing* cures the issue at NLO, but *insufficient* beyond NLO.
- First NLO study with GPD evolution done with APFEL++
- We use High-Energy Factorisation matched to Collinear Factorisation to perform a **high-energy resummation** of the large logarithms of ξ
- *No new non-perturbative ingredients are introduced !*

Conclusion

- Exclusive J/ψ and Υ photoproduction at increasing $W_{\gamma p}$ suffers from *perturbative instabilities at NLO*.
- Similar situation to **inclusive** photoproduction and hadroproduction.
- *Scale fixing* cures the issue at NLO, but *insufficient* beyond NLO.
- First NLO study with GPD evolution done with APFEL++
- We use High-Energy Factorisation matched to Collinear Factorisation to perform a **high-energy resummation** of the large logarithms of ζ
- *No new non-perturbative ingredients are introduced !*
- Like in the **inclusive case**, the matched NLO+HEF results are *stable* and **agree with data** within the (large) theoretical uncertainties.

Conclusion

- Exclusive J/ψ and Υ photoproduction at increasing $W_{\gamma p}$ suffers from *perturbative instabilities at NLO*.
- Similar situation to **inclusive** photoproduction and hadroproduction.
- *Scale fixing* cures the issue at NLO, but *insufficient* beyond NLO.
- First NLO study with GPD evolution done with APFEL++
- We use High-Energy Factorisation matched to Collinear Factorisation to perform a **high-energy resummation** of the large logarithms of ξ
- *No new non-perturbative ingredients are introduced !*
- Like in the **inclusive case**, the matched NLO+HEF results are *stable* and **agree with data** within the (large) theoretical uncertainties.
- The next step is to see **how to fit (gluon) GPDs from such observables**.
- Topic for future synergies between both VAs of STRONG2020:
NLOAccess and PARTONS

Backup

BACKUP SLIDES

Implementation of high-energy resummation

HEF resummation of LLA contributions $\sim \alpha_s^n \ln^{n-1}\left(\frac{x}{\xi}\right)$ *at integrand level* to the imaginary part of the $C_g\left(\frac{\xi}{x}\right)$:

$$C_g^{\text{HEF}}\left(\frac{\xi}{x}\right) = \frac{-i\pi F_{\text{LO}}}{2} \frac{F_{\text{LO}}}{\left(\frac{\xi}{x}\right)} \int_0^\infty d\mathbf{q}_T^2 C_{gi}\left(\frac{\xi}{x}, \mathbf{q}_T^2, \mu_F, \mu_R\right) h(\mathbf{q}_T^2),$$

$$h(\mathbf{q}_T^2) = \frac{M^2}{M^2 + 4\mathbf{q}_T^2}.$$

Implementation of high-energy resummation

Resummation factor, $C_{gi} \left(\frac{\xi}{x}, \mathbf{q}_T^2, \mu_F, \mu_R \right)$ in the *Doubly-Logarithmic Approximation* (DLA) (in order to be consistent with fixed-order evolution of GPD) is given by the Blümlein-Collins-Ellis formula [[hep-ph/9506403](https://arxiv.org/abs/hep-ph/9506403)]

$$C_{gg}^{(DL)} \left(\frac{\xi}{x}, \mathbf{q}_T^2, \mu_F^2, \mu_R^2 \right) = \frac{\hat{\alpha}_s}{\mathbf{q}_T^2} \begin{cases} J_0 \left(2 \sqrt{\hat{\alpha}_s \ln \left(\frac{x}{\xi} \right) \ln \left(\frac{\mu_F^2}{\mathbf{q}_T^2} \right)} \right) & \text{if } \mathbf{q}_T^2 < \mu_F^2, \\ I_0 \left(2 \sqrt{\hat{\alpha}_s \ln \left(\frac{x}{\xi} \right) \ln \left(\frac{\mathbf{q}_T^2}{\mu_F^2} \right)} \right) & \text{if } \mathbf{q}_T^2 > \mu_F^2. \end{cases}$$

\implies resums terms scaling like $(\alpha_s \ln(x/\xi) \ln(\mu_F^2/\mathbf{q}_T^2))^n$ to all orders in perturbation theory.

For the quark channel, the resummation factor is given in the DLA by:

$$C_{gq} \left(\frac{\xi}{x}, \mathbf{q}_T^2, \mu_F^2, \mu_R^2 \right) = \frac{C_F}{C_A} \left[C_{gg} \left(\frac{\xi}{x}, \mathbf{q}_T^2, \mu_F^2, \mu_R^2 \right) - \delta \left(1 - \frac{\xi}{x} \right) \delta(\mathbf{q}_T^2) \right].$$

Implementation of high-energy resummation

Useful representation in Mellin space:

$$C_{gg}^{(\text{DL})}(N, \mathbf{q}_T^2, \mu_F^2, \mu_R^2) = R(\gamma_{gg}) \frac{\gamma_{gg}}{\mathbf{q}_T^2} \left(\frac{\mathbf{q}_T^2}{\mu_F^2} \right)^{\gamma_{gg}}.$$

γ_{gg} is the solution to the equation

$$\frac{\hat{\alpha}_s}{N} \chi(\gamma_{gg}) = 1, \quad \chi(\gamma) = 2\varphi(1) - \varphi(\gamma) - \varphi(1 - \gamma), \quad \varphi(\gamma) = \frac{d \ln \Gamma(\gamma)}{d\gamma}$$

$$\gamma_{gg} = \frac{\hat{\alpha}_s}{N} + \mathcal{O}\left(\frac{\hat{\alpha}_s^4}{N^4}\right), \quad R(\gamma_{gg}) = 1 + \mathcal{O}\left(\hat{\alpha}_s^3\right)$$

DLA \implies *Drop terms in red*: $\gamma_{gg} \rightarrow \gamma_N \equiv \frac{\hat{\alpha}_s}{N}$.

Mellin transform maps logarithms $\ln\left(\frac{x}{\bar{\zeta}}\right)$ to the poles at $N = 0$:

$$\frac{x}{\bar{\zeta}} \ln^{k-1}\left(\frac{x}{\bar{\zeta}}\right) \leftrightarrow \frac{(k-1)!}{N^k}.$$

Shuvaev transform

[0812.3558]

$$H_q(x, \xi) = \int_{-1}^1 dx' \left[\frac{2}{\pi} \operatorname{Im} \int_0^1 \frac{ds}{y(s) \sqrt{1 - y(s)x'}} \right] \frac{d}{dx'} \left(\frac{q(x')}{|x'|} \right),$$

$$H_g(x, \xi) = \int_{-1}^1 dx' \left[\frac{2}{\pi} \operatorname{Im} \int_0^1 \frac{ds(x + \xi(1 - 2s))}{y(s) \sqrt{1 - y(s)x'}} \right] \frac{d}{dx'} \left(\frac{g(x')}{|x'|} \right),$$

$$y(s) = \frac{4s(1 - s)}{x + \xi(1 - 2s)}.$$